PHYSICAL REVIEW B VOLUME 12, NUMBER 8 15 OCTOBER 1975

# Surface roughness and the optical properties of a semi-infinite material; the effect of a dielectric overlayer*

D. L. Mills and A. A. Maradudin
*Department of Physics, University of California, Irvine, California 92664*
*and Xonics Corporation, Van Nuys, California 91406*
(Received 13 January 1975)

We derive expressions for the rate at which radiation is scattered and absorbed because of surface roughness on a semi-infinite material, in the presence of a dielectric overlayer. We confine our attention to the case of normal incidence. A formalism developed in an earlier paper by the present authors is utilized in the discussion. We also present a series of numerical calculations which explore the roughness-induced scattering and absorption of electromagnetic radiation for aluminum overcoated by aluminum oxide, in the ultraviolet region of the spectrum. The position of the reflectivity dip produced by roughness-induced coupling to the surface plasmon is found to shift toward the visible as the thickness of the oxide layer increases. The size of the dip is controlled strongly by the degree of correlation between the roughness on the vacuum-oxide interface, and that on the oxide-substrate interface. Under conditions discussed in the text of the paper, the presence of the oxide layer can greatly enhance the coupling between the incident radiation and surface plasmons.

## I. INTRODUCTION

In the presence of roughness on the surface of a material, light incident on the substance may be scattered away from the specular direction, and roughness-induced absorption can occur. Both effects reduce the reflectivity of the material below the intrinsic value expected for a semi-infinite sample with perfectly smooth surface. The effect is particularly severe for aluminum in the ultraviolet region of the spectrum, since in the presence of surface roughness, the incident light may couple to the surface plasmon with remarkable efficiency.[1]

There has been renewed interest in this problem recently, in part because of the need for highly reflecting mirror materials for use in the construction of cavities for lasers which operate in the ultraviolet region of the spectrum. While aluminum has the highest intrinsic reflectivity of any material in the near ultraviolet, roughness-induced coupling of the incident radiation to surface plasmons can decrease its reflectivity significantly, unless "supersmooth" surfaces are prepared.[2]

Another method that has proved useful in increasing the reflectivity of aluminum films is to overcoat them with a dielectric layer after a very smooth "bare" aluminum surface has been prepared. Such an overlayer will also be present anytime the aluminum has been exposed to an atmosphere that permits oxidation of the surface. One is then led to inquire about the effect of such a dielectric layer on the surface roughness-induced coupling to surface plasmons. While this is a topic that has been explored experimentally,[2-4] we know of no theoretical treatment of the effect of a dielectric overlayer on the roughness-induced scattering and absorption of light.

There seems a critical need for such a theoretical analysis, in our view. From simple considerations, one expects that a dielectric overlayer on a metal such as aluminum will shift the reflectivity dip (produced by the roughness-induced coupling to surface plasmons) toward the visible. One would like to calculate the magnitude of this shift for an overlayer of given thickness, and a specified configuration of surface roughness. Perhaps more important to understand is the relationship of the magnitude of the dip to the nature of the roughness on the overlayer-substrate and overlayer-vacuum interfaces.

The purpose of this paper is to present such a theory by extending our earlier treatment[5] of the surface roughness-induced absorption and scattering of electromagnetic radiation to the case where a dielectric overlayer is present on the surface of the material of interest. In the interest of simplicity, we confine our attention here to the case where the radiation is normally incident on the surface. For this case, we obtain formulas for the angular distribution and polarization of the radiation scattered from the rough surface into the vacuum above the material, for the fraction of the incident radiation flux absorbed within the film, and the fraction of the incident radiation flux absorbed by the substrate material. The treatment is valid in the limit that the amplitude of the surface roughness is very small.

We also present a series of numerical studies of the absorption and scattering of radiation in the near ultraviolet (5–12 eV) by an oxidized surface of aluminum. We find here that the magnitude of the reflectivity dip produced by roughness-induced coupling of the incident radiation to surface plasmons depends very dramatically on the manner in

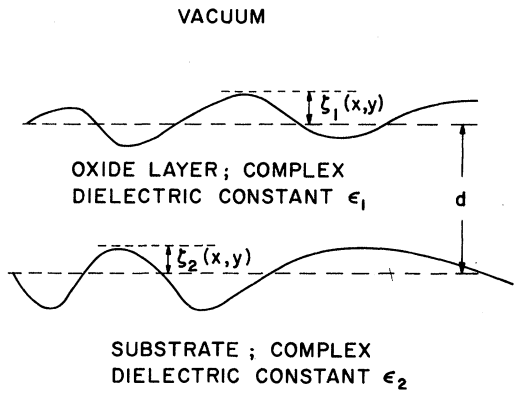


FIG. 1. Illustration of the roughness on the vacuum-oxide interface relative to that on the oxide-substrate interface for the four cases: (a) $\zeta_1 = \zeta_2$ (replicating-film model); (b) $\zeta_1 = -\zeta_2$ (nonuniform-film model); (c) $\langle \zeta_1^2 \rangle = \langle \zeta_2^2 \rangle$, but $\langle \zeta_1 \zeta_2 \rangle = 0$ (random-roughness model); (d) $\zeta_2 \equiv 0$, but $\zeta_1 \neq 0$ (rough-oxide-layer model).

which the roughness on the vacuum-oxide overlayer is correlated with that on the oxide-substrate interface.

Before we proceed with the detailed discussion, we elaborate on this remark a bit. Consider a smooth oxide-vacuum interface parallel to the $x$-$y$ plane located at the position $z = d$, while the smooth oxide-substrate interface is also parallel to the $x$-$y$ plane at $z = 0$. Now roughen each interface, where $\zeta_1(x, y)$ measures the position of the oxide-vacuum interface at the point $x, y$ above the plane $z = d$. Similarly, $\zeta_2(x, y)$ denotes the position of a point on the roughened oxide-substrate interface above the plane $z = 0$. Then if we denote averages over a given interface by angular brackets, we presume $\langle \zeta_1 \rangle = \langle \zeta_2 \rangle = 0$. In our numerical calculations, we examine the following four situations, illustrated schematically in Fig. 1:

(i) $\zeta_1(x, y) \equiv \zeta_2(x, y)$ everywhere. We refer to this as the replicating-film model [Fig. 1(a)].

(ii) $\zeta_1(x, y) = -\zeta_2(x, y)$ everywhere. We call this the nonuniform-film model [Fig. 1(b)]. This might be a crude description of a lumpy oxide overlayer.

(iii) $\langle \zeta_1^2 \rangle = \langle \zeta_2^2 \rangle$, but $\zeta_1(x, y)$ and $\zeta_2(x, y)$ very randomly with respect to each other, so the cross-correlation function $\langle \zeta_1 \zeta_2 \rangle$ vanishes everywhere. We call this the random-roughness model [Fig. 1(c)].

(iv) $\zeta_2 \equiv 0$ but $\zeta_1 \neq 0$; i.e., the oxide-substrate interface is perfectly smooth, but the surface of the oxide is rough. We refer to this as the rough-oxide-layer model [Fig. 1(d)]. It serves as a model of a supersmooth aluminum surface overcoated with a nonuniform oxide film.

When we compare the results of the calculations for the four cases described above, the position of the reflectivity dip is very nearly the same for each case, for an overlayer of given thickness. However, the magnitude of the dip differs markedly in each case. In case (i), the dip moves to lower photon energies as the oxide thickness increases, with no dramatic change in its depth. In case (ii), the dip again moves to lower frequencies, but increases very substantially in depth, i.e., the roughness-induced coupling of the incident photon to the surface plasmon is increased markedly by the presence of the overlayer. In case (iii), there is also considerable enhancement of the roughness-induced coupling to the surface plasmon, although the enhancement is smaller than for case (ii). Finally, for case (iv), once the oxide layer becomes sufficiently thick (say greater than 50 Å), the coupling between the incident radiation and the surface plasmon is greatly decreased.

The above remarks show that in the presence of an oxide film (or a dielectric overlayer), the strength of the roughness-induced coupling to the surface plasmon depends very sensitively not only on the amplitude of the roughness, but also on the manner in which the roughness on the oxide-vacuum interface is correlated with that on the oxide-substrate interface. This is a principal conclusion of the present paper.

The remainder of the paper is organized as follows. In Sec. II, we sketch the derivation of expressions for the roughness-induced scattering of normally incident light, along with the roughness-induced absorption within the film on the substrate. The approach is similar to that employed by us earlier,[5] and although the final formulas are rather cumbersome for the present case, the presentation here is brief. We then present the results of the numerical calculations in Sec. III.

In an Appendix, we describe certain Green's functions of the electromagnetic field equations, for the present geometry. These Green's functions may be employed in a variety of problems. For example, the limiting form of these Green's functions with retardation ignored have formed the basis of a theory of the inelastic scattering of low-energy electrons by electronic excitations in semiconductors.[6]

## II. DERIVATION OF THE THEORETICAL FORMULAS

The geometry which forms the basis of the present paper is illustrated in Fig. 2. In the absence of roughness on the two interfaces, the vacuum-overlayer interface is the plane $z = d$, and the overlayer-substrate interface the plane $z = 0$. In the presence of roughness, the function $\zeta_1(x, y)$ measures the elevation of point $(x, y)$ on the vacuum-overlayer interface relative to the plane $z = d$. Similarly, $\zeta_2(x, y)$ describes the elevation of a point on the overlayer-substrate interface relative

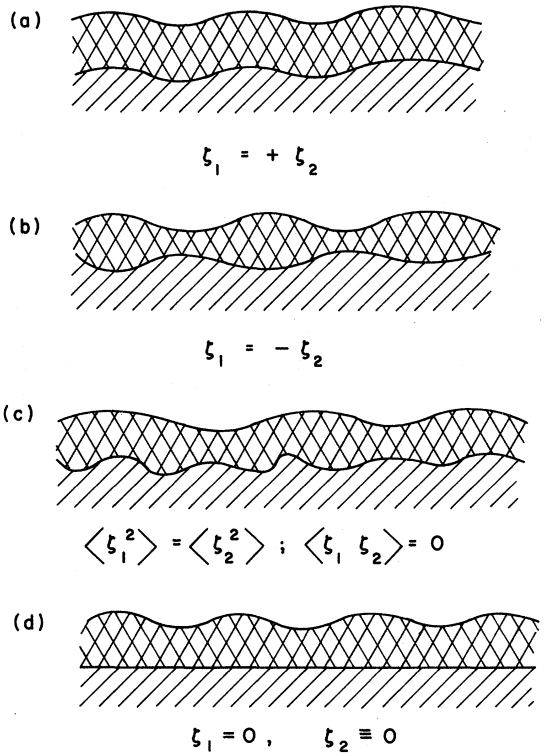


FIG. 2. Geometry considered in the present paper. The thickness of the oxide layer, $\zeta_1(x, y)$, measures the position of a point on the oxide-vacuum interface from the plane $z = d$, and $\zeta_2(x, y)$ measures the position of a point on the oxide-substrate interface from the plane $z = d$.

to the plane $z = 0$. The overlayer material is presumed to be described by the isotropic, complex, frequency-dependent dielectric constant $\epsilon_1$, while the substrate is described by the frequency-dependent dielectric constant $\epsilon_2$, again complex and presumed isotropic. To study the reflectivity of the structure, we look for solutions of Maxwell's equations which vary harmonically with time:

$$\vec{\mathbf{E}}(\vec{\mathbf{x}}, t) = \vec{\mathbf{E}}(\vec{\mathbf{x}}, \omega)\, e^{-i\omega t}, \tag{2.1}$$

where the electric field amplitude $\vec{\mathbf{E}}(\vec{\mathbf{x}}, \omega)$ obeys

$$\vec{\nabla}\times\vec{\nabla}\times\vec{\mathbf{E}}(\vec{\mathbf{x}}, \omega) - (\omega^2/c^2)\epsilon(\vec{\mathbf{x}}, \omega)\vec{\mathbf{E}}(\vec{\mathbf{x}}, \omega) = 0. \tag{2.2}$$

For the geometry of Fig. 2, for the spatially varying dielectric constant, we have

$$\epsilon(\vec{\mathbf{x}}, \omega) = \Theta(z - d - \zeta_1(x, y)) + \epsilon_1\Theta(d + \zeta_1(x, y) - z) \times \Theta(z - \zeta_2(x, y)) + \epsilon_2\Theta(\zeta_2(x, y) - z), \tag{2.3}$$

where in Eq. (2.3), $\Theta(x)$ is the Heaviside step function which assumes the value unity when its argument is positive, and vanishes when its argument is negative.

When both $\zeta_1(x, y)$ and $\zeta_2(x, y)$ are small, we expand the right-hand side of Eq. (2.3) in a Taylor series by means of the well-known expansion

$$\Theta(x + a) = \Theta(x) + a\delta(x) + \cdots, \tag{2.4}$$

where $\delta(x)$ is the Dirac $\delta$ function. Then Eq. (2.3) reads

$$\epsilon(\vec{\mathbf{x}}, \omega) = \epsilon_0(z, \omega) + \Delta\epsilon(\vec{\mathbf{x}}, \omega) \tag{2.5}$$

where

$$\epsilon_0(z, \omega) = \Theta(z - d) + \epsilon_1\Theta(d - z)\Theta(z) + \epsilon_2\Theta(-z) \tag{2.6}$$

and

$$\Delta\epsilon(x, \omega) = \zeta_1(x, y)(\epsilon_1 - 1)\delta(z - d) + (\epsilon_2 - \epsilon_1)\zeta_2(x, y)\delta(z). \tag{2.7}$$

Then Eq. (2.2) may be arranged to read

$$\vec{\nabla}\times\vec{\nabla}\times\vec{\mathbf{E}}(\vec{\mathbf{x}}, \omega) - (\omega^2/c^2)\epsilon_0(z, \omega)\vec{\mathbf{E}}(\vec{\mathbf{x}}, \omega) = (\omega^2/c^2)\Delta\epsilon(\vec{\mathbf{x}}, \omega)\vec{\mathbf{E}}(\vec{\mathbf{x}}, \omega). \tag{2.8}$$

To solve Eq. (2.8) in the limit $\zeta_1(x, y)$ and $\zeta_2(x, y)$ are small, we follow the approach used in our preceding paper.[5] We introduce a set of Green's functions $D_{\mu\nu}(\vec{\mathbf{x}}, \vec{\mathbf{x}}', \omega)$ which satisfy

$$\sum_\mu \left(\frac{\omega^2}{c^2}\epsilon_0(z, \omega)\delta_{\lambda\mu} - \frac{\partial^2}{\partial x_\lambda \partial x_\mu} + \delta_{\lambda\mu}\nabla^2\right) \times D_{\mu\nu}(\vec{\mathbf{x}}\vec{\mathbf{x}}'; \omega) = 4\pi\delta_{\lambda\mu}\delta(\vec{\mathbf{x}} - \vec{\mathbf{x}}'), \tag{2.9}$$

along with boundary conditions appropriate to the present scattering problem.

In terms of these Green's functions, we may rewrite Eq. (2.8) in integral form

$$E_\mu(\vec{\mathbf{x}}, \omega) = E_\mu^{(0)}(\vec{\mathbf{x}}, \omega) - \frac{\omega^2}{4\pi c^2}\sum_\nu \int d^3x'\, D_{\mu\nu}(\vec{\mathbf{x}}, \vec{\mathbf{x}}'; \omega) \times \Delta\epsilon(\vec{\mathbf{x}}', \omega)E_\nu(\vec{\mathbf{x}}', \omega). \tag{2.10}$$

In Eq. (2.10), $E_\nu^{(0)}(\vec{\mathbf{x}}, \omega)$ is a solution of Eq. (2.8) with $\Delta\epsilon(\vec{\mathbf{x}}, \omega) = 0$. The formal structure of Eq. (2.10) is identical to Schrödinger's equation of quantum mechanics, when it is written in integral form.[7] For small $\Delta\epsilon(\vec{\mathbf{x}}, \omega)$, we may generate an approximation analogous to the first Born approximation of quantum mechanics by iterating Eq. (2.10), and approximating the amplitude of the scattered wave $E_\mu^{(s)}(\vec{\mathbf{x}}, \omega)$ by retaining the first term. This gives

$$E_\mu^{(s)}(\vec{\mathbf{x}}, \omega) = \frac{\omega^2}{4\pi c^2}\sum_\nu \int d^3x'\, D_{\mu\nu}(\vec{\mathbf{x}}, \vec{\mathbf{x}}'; \omega) \times \Delta\epsilon(\vec{\mathbf{x}}', \omega)E_\mu^{(0)}(\vec{\mathbf{x}}', \omega). \tag{2.11}$$

The electric field amplitude $E_\mu^{(0)}(\vec{\mathbf{x}}, \omega)$ which appears in the right-hand side of Eq. (2.11) is the electric field associated with the incident field, in the absence of surface roughness. The Green's functions $D_{\mu\nu}(\vec{\mathbf{x}}, \vec{\mathbf{x}}', \omega)$ are constructed in the Appen-

dix of the present paper. Thus, it is a straightforward (but algebraically complex) matter to evaluate the scattered fields in the vacuum, within the overlayer, or within the substrate. We call the reader's attention to the rather extensive discussions in Ref. 5, which explore a number of issues we do not examine here.

As before, since the dielectric function $\epsilon_0(z,\omega)$ which appears on the left-hand side of Eq. (2.9) depends on $z$ only, and not on $x$ and $y$, one may represent the Green's function by the partial Fourier decomposition

$$D_{\mu\nu}(\vec{x},\vec{x}',\omega)=\int\frac{d^2k_{\parallel}}{(2\pi)^2}e^{i\vec{k}_{\parallel}\cdot(\vec{x}_{\parallel}-\vec{x}'_{\parallel})}d_{\mu\nu}(\vec{k}_{\parallel}\omega\,|\,zz'). \quad (2.12)$$

We also write (where $i=1$ or 2)

$$\zeta_i(x,y)=\int\frac{d^2k_{\parallel}}{(2\pi)^2}e^{i\vec{k}_{\parallel}\cdot\vec{x}_{\parallel}}\hat{\xi}_i(\vec{k}_{\parallel}). \quad (2.13)$$

We pressume here that the incident electric field is normally incident on the structure, with electric field parallel to the $\hat{x}$ axis. Then we have

$$E^{(0)}_{\nu}(\vec{x}',\omega)=\delta_{\nu x}E^{(0)}(\omega,z'). \quad (2.14)$$

After these forms are substituted into Eq. (2.11), the scattered field assumes the form[8]

$$E^{(s)}_{\mu}(\vec{x},\omega)=-\frac{\omega^2(\epsilon_1-1)}{2(2\pi)^3c^2}E^{(0)}(\omega,d)\int d^2k_{\parallel}\,e^{i\vec{k}_{\parallel}\cdot\vec{x}_{\parallel}}\times\hat{\xi}_1(\vec{k}_{\parallel})d_{\mu x}(\vec{k}_{\parallel}\omega\,|\,zd)-\frac{\omega^2(\epsilon_2-\epsilon_1)}{2(2\pi)^3c^2}E^{(0)}(\omega,0)\times\int d^2k_{\parallel}\,e^{i\vec{k}_{\parallel}\cdot\vec{x}_{\parallel}}\hat{\xi}_2(\vec{k}_{\parallel})d_{\mu x}(\vec{k}_{\parallel}\omega\,|\,z0). \quad (2.15)$$

From the discussion in the Appendix, the functions $d_{\mu\nu}(\vec{k}_{\parallel}\omega\,|\,zz')$ are related to a second set of functions $g_{\mu\nu}(k_{\parallel}\omega\,|\,zz')$ via the transformation

$$d_{\mu\nu}(\vec{k}_{\parallel}\omega\,|\,zz')=\sum_{\mu',\nu'}S_{\mu'\nu}(\vec{k}_{\parallel})S_{\nu'\nu}(\vec{k}_{\parallel})g_{\mu'\nu'}(k_{\parallel}\omega\,|\,zz'), \quad (2.16)$$

where

$$\vec{k}_{\parallel}=k_x\hat{x}+k_y\hat{y} \quad (2.17)$$

and the matrix $S(\vec{k}_{\parallel})$ is given by

$$\underline{S}(\vec{k}_{\parallel})=\frac{1}{k_{\parallel}}\begin{pmatrix}k_x & k_y & 0\\ -k_y & k_x & 0\\ 0 & 0 & k_{\parallel}\end{pmatrix}. \quad (2.18)$$

One then has the relations

$$d_{xx}(\vec{k}_{\parallel}\omega\,|\,zz')=\frac{k_x^2}{k_{\parallel}^2}g_{xx}(k_{\parallel}\omega\,|\,zz')+\frac{k_y^2}{k_{\parallel}^2}g_{yy}(k_{\parallel}\omega\,|\,zz'), \quad (2.19a)$$

$$d_{yx}(\vec{k}_{\parallel}\omega\,|\,zz')=\frac{k_xk_y}{k_{\parallel}^2}[g_{xx}(k_{\parallel}\omega\,|\,zz')-g_{yy}(k_{\parallel}\omega\,|\,zz')], \quad (2.19b)$$

$$d_{zx}(\vec{k}_{\parallel}\omega\,|\,zz')=\frac{k_x}{k_{\parallel}}g_{zx}(k_{\parallel}\omega\,|\,zz'). \quad (2.19c)$$

To proceed, we now need to evaluate the scattered field in the three distinct regions of interest: in the vacuum above the overlayer, inside the overlayer, and in the substrate. We consider each regime separately.

### A. Scattered fields in the vacuum above the overlayer, and the angular distribution of the scattered radiation

In this regime, we consider the limit $z\to+\infty$, for fixed $z'$. Then the Green's functions $g_{xx}$, $g_{yy}$, and $g_{zx}$ in Eqs. (2.19) have the form

$$g_{yy}(k_{\parallel}\omega\,|\,zz')=\frac{4\pi}{W_1(k_{\parallel},\omega)}E^{>}_y(k_{\parallel}\omega\,|\,z)E^{<}_y(k_{\parallel}\omega\,|\,z'), \quad (2.20a)$$

$$g_{xx}(k_{\parallel}\omega\,|\,zz')=\frac{4\pi}{W_{\parallel}(k_{\parallel},\omega)}E^{>}_x(k_{\parallel}\omega\,|\,z)E^{<}_x(k_{\parallel}\omega\,|\,z'), \quad (2.20b)$$

$$g_{zx}(k_{\parallel}\omega\,|\,zz')=\frac{4\pi}{W_{\parallel}(k_{\parallel},\omega)}E^{>}_z(k_{\parallel}\omega\,|\,z)E^{<}_x(k_{\parallel}\omega\,|\,z'), \quad (2.20c)$$

where for $z>d$, one has

$$E^{>}_y(k_{\parallel}\omega\,|\,z)=E^{>}_z(k_{\parallel}\omega\,|\,z)=e^{ik_0z} \quad (2.21a)$$

and

$$E^{<}_x(k_{\parallel}\omega\,|\,z)=-(k_0/k_{\parallel})\,e^{ik_0z} \quad (2.21b)$$

with

$$k_0=(\omega^2/c^2-k_{\parallel}^2)^{1/2}. \quad (2.22)$$

As discussed in the Appendix, the positive square root is to be chosen in Eq. (2.22), and if $k_{\parallel}>\omega/c$, we choose

$$\mathrm{Im}(k_0)>0.$$

The remaining quantities in Eqs. (2.20) and Eqs. (2.21) are defined in the Appendix.

The scattered electric field has the form

$$E^{(s)}_{\mu}(\vec{x},\omega)=\int d^2k_{\parallel}\,\mathcal{E}_{\mu}(\vec{k}_{\parallel},\omega)\,e^{i\vec{k}\cdot\vec{x}}, \quad (2.23)$$

where in Eq. (2.23),

$$\vec{k}=\vec{k}_{\parallel}+\hat{z}k_0. \quad (2.24)$$

It is a short exercise to show that the time average of the Poynting vector, $\langle\vec{S}\rangle$, may be cast into the form

$$\langle\vec{S}\rangle=\frac{c^2}{8\pi\omega}\mathrm{Re}\int d^2k_{\parallel}\,d^2k'_{\parallel}\,e^{i(\vec{k}-\vec{k}'^{*})\cdot\vec{x}}\times\{\vec{k}[\vec{\mathcal{E}}^{*}(\vec{k}'_{\parallel}\omega)\cdot\vec{\mathcal{E}}(\vec{k}_{\parallel}\omega)]-\vec{\mathcal{E}}(\vec{k}_{\parallel}\omega)[\vec{k}\cdot\vec{\mathcal{E}}^{*}(\vec{k}'_{\parallel}\omega)]\}. \quad (2.25)$$

We are interested here in the energy radiated into

the vacuum. Thus, we confine our attention to the contributions to the integral from the regions $k_{\parallel} < \omega/c$, $k'_{\parallel} < \omega/c$. As explained earlier,[5] the regions with $k_{\parallel} > \omega/c$ describe scattered energy which is confined to the near vicinity of the surface, and which propagates parallel to it (i.e., stored in surface plasmons excited by the incident radiation, for example). The regions $k_{\parallel} > \omega/c$, $k'_{\parallel} > \omega/c$ give contributions to the energy flux which are small,[5] unless the surface plasmon in mean free path is comparable to the linear dimensions of the region illuminated by the incident beam.

We may calculate the Poynting vector by inserting the amplitudes of the scattered fields into $\langle \vec{S} \rangle$, and then averaging over the distribution of surface roughness, as we did before. The calculation proceeds along very similar lines to our earlier work.

We comment on one point, however. When one averages over the distribution of surface roughness, one encounters averages of the form $\langle \hat{\zeta}_i(\vec{k}_{\parallel})^* \times \zeta_j(\vec{k}'_{\parallel}) \rangle$. The two functions $\langle \hat{\zeta}_1(\vec{k}_{\parallel})^* \hat{\zeta}_1(\vec{k}'_{\parallel}) \rangle$ and $\langle \hat{\zeta}_2(\vec{k}_{\parallel})^* \hat{\zeta}_2(\vec{k}'_{\parallel}) \rangle$ describe the nature of the roughness on the vacuum-overlayer and overlayer-substrate interfaces, respectively. In general, the "off-diagonal" averages $\langle \hat{\zeta}_1(\vec{k}_{\parallel})^* \hat{\zeta}_2(\vec{k}'_{\parallel}) \rangle$ and $\langle \hat{\zeta}_2(\vec{k}_{\parallel})^* \hat{\zeta}_1(\vec{k}'_{\parallel}) \rangle$ will be also nonzero. These functions contain information about the manner in which the roughness on the vacuum-overlayer interface is *correlated* with that on the overlayer-substrate interface. These functions will vanish only if the roughness on the outermost interface is distributed randomly relative to that on the innermost interface, a possibility that seems unlikely for a thin overlayer.

By a straightforward generalization of our earlier definitions, we write

$$\langle \hat{\zeta}_i^*(\vec{k}_{\parallel}) \zeta_j(\vec{k}'_{\parallel}) \rangle = (2\pi)^2 \delta(\vec{k}_{\parallel} - \vec{k}'_{\parallel}) \delta_i \delta_j g_{ij}(\vec{k}_{\parallel}), \quad (2.26)$$

where

$$g_{ij}(\vec{k}_{\parallel}) = \frac{1}{\delta_i \delta_j} \int d^2 r_{\parallel} \, e^{-i\vec{k}_{\parallel} \cdot \vec{r}_{\parallel}} \langle \zeta_i(0) \zeta_j(\vec{r}_{\parallel}) \rangle. \quad (2.27)$$

In Eq. (2.26) and Eq. (2.27), the quantities $\delta_1$ and $\delta_2$ are the root-mean-square roughness amplitudes for the vacuum-overlayer interface, and the overlayer-substrate interface, respectively, i.e.,

$$\delta_1 = \langle \zeta_1^2 \rangle^{1/2} \quad (2.28a)$$

and

$$\delta_2 = \langle \zeta_2^2 \rangle^{1/2}. \quad (2.28b)$$

It follows from this definition that

$$\int \frac{d^2 k_{\parallel}}{4\pi^2} g_{11}(\vec{k}_{\parallel}) = \int \frac{d^2 k_{\parallel}}{4\pi^2} g_{22}(\vec{k}_{\parallel}) = 1, \quad (2.29)$$

while no simple normalization requirement exists for $g_{12}(\vec{k}_{\parallel})$ or $g_{21}(\vec{k}_{\parallel})$, although necessarily $g_{12}(\vec{k}_{\parallel}) = g_{21}(\vec{k}_{\parallel})^*$.

The overlayer roughness configurations illustrated in Fig. 1 can be seen to correspond to particular choices of $g_{12}(\vec{k}_{\parallel})$. For example, the replicating-film model of Fig. 1(a) corresponds to the choice $g_{11}(\vec{k}_{\parallel}) = g_{22}(\vec{k}_{\parallel}) = g_{12}(\vec{k}_{\parallel})$, and the nonuniform-film model of Fig. 1(b) to the choice $g_{11}(\vec{k}_{\parallel}) = g_{22}(\vec{k}_{\parallel}) = -g_{12}(\vec{k}_{\parallel})$.

With the above remarks and our preceding discussion in hand, one may construct expressions for the angular distribution of the scattered energy flux. We shall simply quote the results here, since the algebraic manipulations are lengthy and offer no enlightenment.

We let $(df_s/d\Omega)d\Omega$ be the fraction of the incident radiation (recall we consider only normal incidence here) scattered into final states with $s$ polarization, directed toward the solid angle $d\Omega$. In a similar fashion, $(df_p/d\Omega)$ describes the angular distribution of radiation of $p$ polarization. The direction of the outgoing radiation is described by the spherical angles $\theta_s$ and $\varphi_s$, where $\varphi_s$ is measured from the $x$ axis.

Before we write down the final expressions, we define the following quantities:

$$\kappa_1 = (\epsilon_1 - \sin^2\theta_s)^{1/2}, \quad \mathrm{Im}(\kappa_1) > 0 \quad (2.30a)$$

$$\kappa_2 = (\epsilon_2 - \sin^2\theta_s)^{1/2}, \quad \mathrm{Im}(\kappa_2) > 0 \quad (2.30b)$$

$$d_s(\theta_s, \omega) = (\kappa_2 + \cos\theta_s) \cos[(\omega/c)\kappa_1 d] - (i/\kappa_1) \times (\kappa_1^2 + \kappa_2 \cos\theta_s) \sin[(\omega/c)\kappa_1 d], \quad (2.30c)$$

$$\mathcal{S}_s(\theta_s, \omega) = \cos[(\omega/c)\kappa_1 d] - i(\kappa_2/\kappa_1) \sin[(\omega/c)\kappa_1 d], \quad (2.30d)$$

$$d_p(\theta_s, \omega) = (\epsilon_2 \cos\theta_s + \kappa_2) \cos[(\omega/c)\kappa_1 d] - i\left(\cos\theta_s \epsilon_1 \frac{\kappa_2}{\kappa_1} + \frac{\epsilon_2}{\epsilon_1}\kappa_1\right) \sin[d(\omega/c)\kappa_1], \quad (2.30e)$$

$$\mathcal{S}_p(\theta_s, \omega) = \cos\left(\frac{\omega}{c}\kappa_1 d\right) - i\frac{\epsilon_2 \kappa_1}{\epsilon_1 \kappa_2} \sin\left(\frac{\kappa}{c}\kappa_1 d\right). \quad (2.30f)$$

We then have[9]

$$\frac{df_s(\theta, \varphi_s)}{d\Omega} = \frac{\omega^4}{\pi^2 c^4} \frac{\cos^2\theta_s \sin^2\varphi_s}{|d_s(\theta_s, \omega)|^2 |d_s(0, \omega)|^2} \{\delta_1^2 |\epsilon_1 - 1|^2 |\mathcal{S}_s(\theta_s, \omega)|^2 |\mathcal{S}_s(0, \omega)|^2 g_{11}(\vec{k}_{\parallel}) + \delta_2^2 |\epsilon_2 - \epsilon_1|^2 g_{22}(\vec{k}_{\parallel}) + 2\delta_1 \delta_2 \mathrm{Re}[(\epsilon_1^* - 1)(\epsilon_2 - \epsilon_1) \mathcal{S}_s^*(0, \omega) \mathcal{S}_s(\theta_s, \omega) g_{12}(\vec{k}_{\parallel})]\} \quad (2.31)$$

and

$$\frac{df_p(\theta_s,\varphi_s)}{d\Omega_p}=\frac{\omega^4}{\pi^2c^4}\frac{\cos^2\theta_s\cos^2\varphi_s\,|\kappa_2|^2}{|d_p(\theta_s,\omega)|^2|d_s(0,\omega)|^2}\{\delta_1^2|\epsilon_1-1|^2|\mathcal{E}_p(\theta_s,\omega)|^2|\mathcal{E}_s(0,\omega)|^2 g_{11}(\vec{k}_\parallel)+\delta_2^2|\epsilon_2-\epsilon_1|^2 g_{22}(\vec{k}_\parallel)$$
$$+2\delta_1\delta_2\,\mathrm{Re}[(\epsilon_1^*-1)(\epsilon_2-\epsilon_1)\mathcal{E}_s^*(0,\omega)\mathcal{E}_p(\theta_s,\omega)g_{12}(\vec{k}_\parallel)]\}\ . \tag{2.32}$$

In Eq. (2.31) and Eq. (2.32), $\vec{k}_\parallel$ is the projection of the wave vector of the scattered wave vector on a plane parallel to the surface. Thus, the magnitude of $\vec{k}_\parallel$ is given by

$$|\vec{k}_\parallel|=(\omega/c)\sin\theta_s. \tag{2.33}$$

### B. Scattered electric fields within the overlayer, and the fraction of the incident energy absorbed within the overlayer

To compute the scattered electric field within the film, we may use Eq. (2.15), with the Green's functions $d_{\mu x}(\vec{k}_\parallel\omega|zd)$ and $d_{\mu x}(\vec{k}_\parallel\omega|z0)$ given by Eq. (2.19).

If we define (as in the Appendix)

$$k_1=[(\omega^2/c^2)\epsilon_1-k_\parallel^2]^{1/2},\quad \mathrm{Im}(k_1)<0, \tag{2.34}$$

then the electric field within the film has the form

$$E_\mu^{(s)}(\vec{x},\omega)=\int d^2k_\parallel\, e^{i\vec{k}_\parallel\cdot\vec{x}_\parallel}[\mathcal{E}_\mu^{(+)}(\vec{k}_\parallel,\omega)\,e^{+ik_1z}+\mathcal{E}_\mu^{(-)}(\vec{k}_\parallel,\omega)\,e^{-ik_1z}], \tag{2.35}$$

where after some algebra, one finds

$$\mathcal{E}_x^{(\sigma)}(\vec{k}_\parallel,\omega)=-\frac{\omega^2(\epsilon_1-1)}{(2\pi)^2c^2}E^{(0)}(\omega,d)\,e^{ik_0d}\hat{\xi}_1(\vec{k}_\parallel)\left(\sigma\frac{k_0k_1k_x^2}{W_\parallel(k_\parallel,\omega)k_\parallel^4}C_\sigma^{(\parallel)}+\frac{k_y^2}{k_\parallel^2W_\perp(k_\parallel,\omega)}C_\sigma^{(\perp)}\right)$$
$$-\frac{\omega^2(\epsilon_2-\epsilon_1)}{(2\pi)^2c^2}E^{(0)}(\omega,0)\hat{\xi}_2(\vec{k}_\parallel)\left(\sigma\frac{k_1k_2k_x^2}{k_\parallel^4W_\parallel(k_\parallel,\omega)}A_\sigma^{(\parallel)}+\frac{k_y^2}{k_\parallel^2W_\perp(k_\parallel,\omega)}A_\sigma^{(\perp)}\right), \tag{2.36}$$

$$\mathcal{E}_y^{(\sigma)}(\vec{k}_\parallel,\omega)=-\frac{\omega^2(\epsilon_1-1)}{(2\pi)^2c^2}E^{(0)}(\omega,d)\,e^{ik_0d}\hat{\xi}_1(\vec{k}_\parallel)\frac{k_xk_y}{k_\parallel^2}\left(\sigma\frac{k_0k_1}{k_\parallel^2W_\parallel(k_\parallel,\omega)}C_\sigma^{(\parallel)}-\frac{1}{W_\perp(k_\parallel,\omega)}C_\sigma^{(\perp)}\right)$$
$$-\frac{\omega^2(\epsilon_2-\epsilon_1)}{(2\pi)^2c^2}E^{(0)}(\omega,0)\hat{\xi}_2(\vec{k}_\parallel)\frac{k_xk_y}{k_\parallel^2}\left(\sigma\frac{k_1k_2}{k_\parallel^2W_\parallel(k_\parallel,\omega)}A_\sigma^{(\parallel)}-\frac{1}{W_\perp(k_\parallel,\omega)}A_\sigma^{(\perp)}\right)\ , \tag{2.37}$$

$$\mathcal{E}_z^{(\sigma)}(\vec{k}_\parallel,\omega)=+\frac{\omega^2(\epsilon_1-1)}{(2\pi)^2c^2}E^{(0)}(\omega,d)\,e^{ik_0d}\hat{\xi}_1(\vec{k}_\parallel)\frac{k_0k_x}{k_\parallel^2W_\parallel(k_\parallel,\omega)}C_\sigma^{(\parallel)}+\frac{\omega^2(\epsilon_2-\epsilon_1)}{(2\pi)^2c^2}E^{(0)}(\omega,0)\hat{\xi}_2(\vec{k}_\parallel)\frac{k_xk_y}{k_\parallel^2W_\parallel(k_\parallel,\omega)}A_\sigma^{(\parallel)}. \tag{2.38}$$

In Eqs. (2.36), (2.37), and (2.38), we have as in the Appendix,

$$k_2=[(\omega^2/c^2)\epsilon_2-k_\parallel^2]^{1/2}\,\mathrm{Im}(k_2)<0, \tag{2.39}$$

$$k_0=[(\omega^2/c^2)-k_\parallel^2]^{1/2}\,\mathrm{Im}(k_0)\geq 0. \tag{2.40}$$

The coefficients $C_\pm^{(\parallel)}$, $C_\pm^{(\perp)}$, etc. are given by

$$C_\sigma^{(\perp)}=\tfrac{1}{2}(1+\sigma k_2/k_1), \tag{2.41a}$$

$$C_\sigma^{(\parallel)}=\tfrac{1}{2}(\epsilon_2/\epsilon_1+\sigma k_2/k_1), \tag{2.41b}$$

$$A_\sigma^{(\perp)}=\tfrac{1}{2}(1+\sigma k_0/k_1)\,e^{ik_0d}\,e^{-i\sigma k_1d}, \tag{2.41c}$$

$$A_\sigma^{(\parallel)}=\tfrac{1}{2}(1/\epsilon_1+\sigma k_0/k_1)\,e^{ik_0d}\,e^{-i\sigma k_1d}. \tag{2.41d}$$

It is now a straightforward, but tedious matter to evaluate the fraction of the incident radiation absorbed by the overlayer. By symmetry, the only component of the Poynting vector which has a nonvanishing value is the $z$ component $\langle S_z\rangle$. The rate at which energy is dissipated in the film is then $L_xL_y(\langle S_z\rangle|_{z=0}-\langle S_z\rangle|_{z=d})$, where $L_xL_y$ is the area illuminated by the incident beam. We calculate this quantity, and divide by the rate at which incident energy strikes the surface to form an expression for the fraction $f^{(1)}$ of the incident energy absorbed by the overlayer. The quantity $f^{(1)}$ has the form

$$f^{(1)}=\sum_{\sigma=\pm1}\sum_{\sigma'=\pm1}f_{\sigma\sigma'}^{(1)}, \tag{2.42}$$

where

$$f_{\sigma\sigma'}^{(1)}=\frac{\omega}{4\pi^2c}\frac{1}{|d_s(0,\omega)|^2}\mathrm{Re}\left(\int d^2k_\parallel\,(1-e^{id(\sigma k_1-\sigma'k_1^*)})\left\{\delta_1^2|\epsilon_1-1|^2|\mathcal{E}_s(0,\omega)|^2g_\parallel(\vec{k}_\parallel)\right.\right.$$
$$\left.\left.\times\left[\sigma'\cos^2\varphi_s\frac{c^2}{\omega^2}\frac{|k_0|^2(k_1|k_1|^2+k_\parallel^2k_1^*)}{|d_p(k_\parallel,\omega)|^2}\left(\frac{\epsilon_2^*}{\epsilon_1^*}+\sigma'\frac{k_2^*}{k_1^*}\right)\left(\frac{\epsilon_2}{\epsilon_1}+\sigma\frac{k_0}{k_1}\right)+\sigma\sin^2\varphi_s\frac{\omega^2}{c^2}\frac{k_1}{|d_s(k_\parallel,\omega)|^2}\left(1+\sigma'\frac{k_2^*}{k_1^*}\right)\left(1+\sigma\frac{k_2}{k_1}\right)\right]\right.$$

$$+\delta_2^2|\epsilon_2-\epsilon_1|^2 g_{22}(\vec{k}_\parallel)\, e^{-i(\sigma k_1-\sigma k_1^*)d}\left[\sigma'\cos^2\varphi_s\frac{c^2}{\omega^2}\frac{|k_2|^2(k_1|k_1|^2+k_\parallel^2k_1^*)}{|d_p(k_\parallel,\omega)|^2}\left(\frac{1}{\epsilon_1^*}+\sigma'\frac{k_0^*}{k_1^*}\right)\left(\frac{1}{\epsilon_1}+\sigma\frac{k_0}{k_1}\right)\right.$$

$$\left.+\sigma\sin^2\varphi_s\frac{\omega^2}{c^2}\frac{k_1}{|d_s(k_\parallel,\omega)|^2}\left(1+\sigma'\frac{k_0^*}{k_1^*}\right)\left(1+\sigma\frac{k_0}{k_1}\right)\right]+\delta_1\delta_2(\epsilon_2-\epsilon_1)(\epsilon_1^*-1)\mathcal{S}_s^*(0,\omega)\,e^{-i\sigma k_1 d}g_{12}(k_\parallel)$$

$$\times\left[\sigma'\cos^2\varphi_s\frac{c^2}{\omega^2}\frac{k_0^*(k_1|k_1|^2+k_\parallel^2k_1^*)k_2}{|d_p(k_\parallel,\omega)|^2}\left(\frac{\epsilon_2^*}{\epsilon_1^*}+\sigma'\frac{k_2^*}{k_1^*}\right)\left(\frac{1}{\epsilon_1}+\sigma\frac{k_0}{k_1}\right)+\sigma\sin^2\varphi_s\frac{\omega^2}{c^2}\frac{k_1}{|d_s(k_\parallel,\omega)|^2}\left(1+\sigma'\frac{k_2^*}{k_1^*}\right)\left(1+\sigma\frac{k_0}{k_1}\right)\right]$$

$$+\delta_1\delta_2(\epsilon_2^*-\epsilon_1^*)(\epsilon_1-1)\mathcal{S}_s(0,\omega)\,e^{+i\sigma' k_1^* d}g_{12}^*(\vec{k}_\parallel)\left[\sigma'\cos^2\varphi_s\frac{c^2}{\omega^2}\frac{k_0(k_1|k_1|^2+k_\parallel^2k_1^*)k_2^*}{|d_p(k_\parallel,\omega)|^2}\left(\frac{1}{\epsilon_1^*}+\sigma'\frac{k_0^*}{k_1^*}\right)\left(\frac{\epsilon_2}{\epsilon_1}+\sigma\frac{k_2}{k_1}\right)\right.$$

$$\left.\left.+\sigma\sin^2\varphi_s\frac{\omega^2}{c^2}\frac{k_1}{|d_s(k_\parallel,\omega)|^2}\left(1+\sigma'\frac{k_0^*}{k_1^*}\right)\left(1+\sigma\frac{k_2}{k_1}\right)\right]\right\}\Big)\,.$$

In Eq. (2.42), we have

$$d_s(k_\parallel,\omega)=(k_0-k_2)\cos(k_1d)-i\left(k_1-\frac{k_0k_2}{k_1}\right)\sin(k_1d) \tag{2.43}$$

and

$$d_p(k_\parallel,\omega)=(\epsilon_2k_0-k_2)\cos(k_1d)-i\left(\frac{\epsilon_2k_1}{\epsilon_1}-\epsilon_1\frac{k_2k_0}{k_1}\right)\sin(k_1d). \tag{2.44}$$

The definitions of the remaining quantities may be found earlier in the present section.

### C. Scattered electric fields within the substrate, and the fraction of the incident energy absorbed within the substrate

We evaluate the scattered electric field within the substrate through the use once again of Eq. (2.15) in concert with Eqs. (2.19). Now we require the Green's functions for $z<0$, $z<z'$. In this regime we have

$$g_{xx}(k_\parallel\omega\,|\,zz')=\frac{4\pi}{W_\parallel(k_\parallel,\omega)}E_x^<(k_\parallel\omega\,|\,z)E_x^>(k_\parallel\omega\,|\,z'), \tag{2.45a}$$

$$g_{yy}(k_\parallel\omega\,|\,zz')=\frac{4\pi}{W_\perp(k_\parallel,\omega)}E_y^<(k_\parallel\omega\,|\,z)E_y^>(k_\parallel\omega\,|\,z'), \tag{2.45b}$$

$$g_{zx}(k_\parallel\omega\,|\,zz')=\frac{4\pi}{W_\parallel(k_\parallel,\omega)}E_z^<(k_\parallel\omega\,|\,z)E_x^>(k_\parallel\omega\,|\,z'), \tag{2.45c}$$

where

$$E_x^<(k_\parallel\omega\,|\,z)=-(k_2/k_\parallel)\,e^{ik_2z}, \tag{2.46a}$$

$$E_y^<(k_\parallel\omega\,|\,z)=e^{ik_2z}, \tag{2.46b}$$

$$E_z^<(k_\parallel\omega\,|\,z)=e^{ik_2z}. \tag{2.46c}$$

The scattered field in the substrate then assumes the form

$$E_\mu^{(s)}(\vec{x},\omega)=\int d^2k_\parallel\, e^{i\vec{k}_\parallel\cdot\vec{x}_\parallel}\,e^{ik_2z}\,\mathcal{S}_\mu^{(2)}(\vec{k},\omega), \tag{2.47}$$

where the explicit form of the quantities $\mathcal{S}_\mu^{(2)}(\vec{k}_\parallel,\omega)$ is

$$\mathcal{S}_x^{(2)}(\vec{k}_\parallel,\omega)=+\frac{\omega^2(\epsilon_1-1)}{(2\pi)^2c^2}E^{(0)}(\omega,d)\hat{\xi}_1(\vec{k}_\parallel)\left(\frac{k_x^2k_2}{k_\parallel^3W_\parallel(k_\parallel,\omega)}E_x^>(k_\parallel\omega\,|\,d)-\frac{k_y^2}{W_\perp(k_\parallel,\omega)k_\parallel^2}E_y^>(k_\parallel\omega\,|\,d)\right)$$

$$+\frac{\omega^2(\epsilon_2-\epsilon_1)}{(2\pi)^2c^2}E^{(0)}(\omega,0)\hat{\xi}_2(\vec{k}_\parallel)\left(\frac{k_x^2k_2E_x^>(k_\parallel\omega\,|\,0)}{k_\parallel^3W_\parallel(k_\parallel,\omega)}-\frac{k_y^2E_y^>(k_\parallel\omega\,|\,0)}{k_\parallel^2W_\perp(k_\parallel,\omega)}\right), \tag{2.48a}$$

$$\mathcal{S}_y^{(2)}(\vec{k}_\parallel\omega)=\frac{\omega^2(\epsilon_1-1)}{(2\pi)^2c^2}E^{(0)}(\omega,d)\hat{\xi}_1(k_\parallel)\frac{k_xk_y}{k_\parallel^2}\left(\frac{k_2E_x^>(k_\parallel\omega\,|\,d)}{k_\parallel W_\parallel(k_\parallel,\omega)}+\frac{E_y^>(k_\parallel\omega\,|\,d)}{W_\perp(k_\parallel,\omega)}\right)$$

$$+\frac{\omega^2(\epsilon_2-\epsilon_1)}{(2\pi)^2c^2}E^{(0)}(\omega,0)\hat{\xi}_2(k_\parallel)\frac{k_xk_y}{k_\parallel^2}\left(\frac{k_2E_x^>(k_\parallel\omega\,|\,0)}{k_\parallel W_\parallel(k_\parallel,\omega)}+\frac{E_y^>(k_\parallel\omega\,|\,0)}{W_\perp(k_\parallel,\omega)}\right), \tag{2.48b}$$

$$\mathcal{S}_z^{(2)}(\vec{k}_\parallel,\omega)=-\frac{\omega^2(\epsilon_1-1)}{(2\pi)^2c^2}E^{(0)}(\omega,d)\hat{\xi}_1(\vec{k}_\parallel)\frac{k_xE_x^>(k_\parallel\omega\,|\,d)}{k_\parallel W_\parallel(k_\parallel,\omega)}-\frac{\omega^2(\epsilon_2-\epsilon_1)}{(2\pi)^2c^2}E^{(0)}(\omega,0)\hat{\xi}_2(\vec{k}_\parallel)\frac{k_xE_x^>(k_\parallel\omega\,|\,0)}{k_\parallel W_\parallel(k_\parallel,\omega)}\,. \tag{2.48c}$$

In Ref. 5, it was argued that in the limit that the mean free path of the surface plasmon is short compared to the linear size of the region of the surface illuminated by the incident beam, then the dominant contribution to the energy absorption by the substrate comes from the energy flow in the direction normal to the surface. This rate is equal to $L_xL_y\langle S_z\rangle|_{z=0_-}$, where again $L_xL_y$ is the area of the surface illuminated by the incident beam. It is straightforward to compute this quantity, and divide it by the energy/unit time that strikes the surface to obtain the fraction $f^{(2)}$ of the incident energy absorbed within the substrate. When this is done, we find the following expression:

$$f^{(2)} = \frac{\omega}{\pi^2 c}\frac{1}{|d_s(0,\omega)|^2}\int d^2k_{\parallel}\,|\mathrm{Re}(k_2)|\left(\cos^2\varphi_s \frac{c^2|k_0|^2(k_{\parallel}^2+|k_2|^2)}{\omega^2|d_p(k_{\parallel},\omega)|^2}\{\delta_1^2|\epsilon_1-1|^2|\mathcal{S}_s(0,\omega)|^2 g_{11}(\vec{k}_{\parallel})\right.$$

$$+2\delta_1\delta_2\,\mathrm{Re}[(\epsilon_1^*-1)(\epsilon_2-\epsilon_1)\mathcal{S}_s^*(0,\omega)\epsilon_p(k_{\parallel},\omega)g_{12}(k_{\parallel})]+\delta_2^2|\epsilon_2-\epsilon_1|^2|\epsilon_p(k_{\parallel},\omega)|^2 g_{22}(\vec{k}_{\parallel})\}$$

$$+\sin^2\varphi_s\frac{\omega^2}{c^2}\frac{1}{|d_s(k_{\parallel},\omega)|^2}\{\delta_1^2|\epsilon_1-1|^2|\mathcal{S}_s(0,\omega)|^2 g_{11}(\vec{k})+2\delta_1\delta_2\,\mathrm{Re}[(\epsilon_1^*-1)(\epsilon_2-\epsilon_1)\mathcal{S}_s^*(0,\omega)\epsilon_s(k_{\parallel},\omega)g_{12}(\vec{k}_{\parallel})]$$

$$\left.+\delta_2^2|\epsilon_2-\epsilon_1|^2|\epsilon_s(k_{\parallel},\omega)|^2 g_{22}(\vec{k}_{\parallel})\}\right). \tag{2.49}$$

In Eq. (2.49), we have introduced the quantities

$$\epsilon_s(k_{\parallel}\omega) = \cos(k_1 d) - i(k_0/k_1)\sin(k_1 d), \tag{2.50}$$

$$\epsilon_p(k_{\parallel}\omega) = \cos(k_1 d) - i(k_1/\epsilon_1 k_0)\sin(k_1 d). \tag{2.51}$$

## III. NUMERICAL CALCULATIONS

In this section, we present the results of a set of numerical calculations of the change in reflectivity of the structure, in the presence of surface roughness.

To carry out these calculations, we require values of the complex dielectric constant $\epsilon_1$ of the overlayer, and the complex dielectric constant $\epsilon_2$ of the substrate. We have chosen to carry out the calculations for aluminum metal overcoated with an oxide film. For the dielectric constant of the overlayer, we have employed the dielectric constant of $Al_2O_3$ films reported by Arakawa and Williams.[10] These data show that the dielectric constant of $Al_2O_3$ is real below photon energies of $\approx 8$ eV, and absorption sets in for photon energies higher than this value. For the dielectric constant $\epsilon_2$ of the substrate, we have employed the values for aluminum reported by Ehrenreich, Philipp, and Segall.[11]

We also require values for the correlation functions $g_{11}(\vec{k})$, $g_{22}(\vec{k}_{\parallel})$, and $g_{12}(\vec{k})$. We shall restrict our attention to the four model situations depicted in Fig. 1. In each case, a simple relation exists between the three correlation functions; so we only need specify one of them to proceed. The relations are as follows.

(i) The replicating-film model [Fig. 1(a)]. Here we have $\zeta_1(x,y) = \zeta_2(x,y)$ everywhere so that

$$g_{11}(\vec{k}_{\parallel}) = g_{22}(\vec{k}_{\parallel}) = g_{12}(\vec{k}_{\parallel}) \tag{3.1}$$

and also

$$\delta_1 = \delta_2 \ . \tag{3.2}$$

(ii) The nonuniform-film model [Fig. 1(b)]. Here we have $\zeta_1(x,y) = -\zeta_1(x,y)$ everywhere. Then

$$g_{11}(\vec{k}_{\parallel}) = g_{22}(\vec{k}_{\parallel}) = -g_{12}(\vec{k}_{\parallel}) \tag{3.3}$$

and again

$$\delta_1 = \delta_2 \ . \tag{3.4}$$

(iii) The random-roughness model [Fig. 1(c)]. In this model, we presume that the roughness on the vacuum-oxide interface is uncorrelated with that on the oxide-substrate interface. This means that

$$g_{12}(\vec{k}_{\parallel}) = 0 \ , \tag{3.5}$$

while $g_{11}(\vec{k}_{\parallel})$ and $g_{22}(\vec{k}_{\parallel})$ bear no simple relation to each other, in general. For simplicity, however, we shall choose

$$g_{11}(\vec{k}_{\parallel}) = g_{22}(\vec{k}_{\parallel}) \tag{3.6}$$

and

$$\delta_1 = \delta_2 \tag{3.7}$$

for this model, while the condition in Eq. (3.5) holds also.

(iv) The rough-oxide-layer model. We presume the oxide-substrate interface is perfectly smooth, while the interface between the oxide film and the vacuum is rough. This means that $\zeta_2(x,y) = 0$ everywhere; so we have the conditions

$$g_{22}(\vec{k}_{\parallel}) = g_{12}(\vec{k}_{\parallel}) = 0, \tag{3.8}$$

$$g_{11}(\vec{k}_{\parallel}) \neq 0 \ . \tag{3.9}$$

Each of the four models described above requires knowledge of one correlation function $g_{11}(\vec{k}_{\parallel})$, and the remaining correlation functions may be obtained from it. As in our earlier calculations, we choose a Gaussian for $g_{11}(\vec{k}_{\parallel})$:

$$g_{11}(\vec{k}_{\parallel}) = \pi a^2 \exp(-\tfrac{1}{4}a^2 k_{\parallel}^2) \ . \tag{3.10}$$

The parameter $a$ is the transverse correlation length. It is a measure of the average distance between neighboring peaks on the rough surface.

To begin, we calculate the change in reflectivity for a rough surface of pure aluminum, with no oxide overlayer present. While we presented similar calculations in our earlier work, in the present calculation we have chosen a value for the

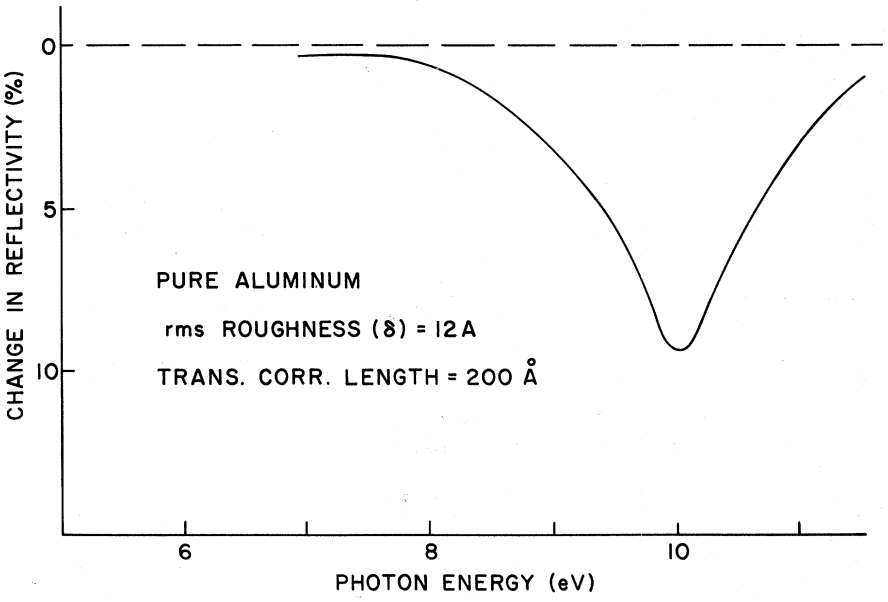


FIG. 3. Change in reflectivity for a rough aluminum surface, for the case where the transverse correlation length is chosen to be 200 Å, and the rms amplitude of the surface roughness is 12 Å.

transverse correlation length which provides a rough fit to the data reported by Endriz and Spicer.[12] These authors have completed an extensive series of experimental studies of the effect of roughness on the reflectivity of aluminum in the ultraviolet.

In their paper, Endriz and Spicer have also provided detailed fits to their data. However, in their fitting procedure, they employed theoretical expressions which have appeared in the literature,[13] but which are in error.[5,14] In our present calculations, we have not attempted to obtain the kind of detailed quantitative fit to the data attempted by Endriz and Spicer. Our interest here is in a calculation which provides a reasonable qualitative fit.

We find that if we choose the transverse correlation length $a = 200$ Å, we obtain results rather similar to the experimental data. In Fig. 3, we present our results, for the case where the root-mean-square height of the roughness (the parameter $\delta$) is chosen to be 12 Å. The dominant contribution to the roughness-induced change in reflectivity comes from roughness-induced coupling to the surface plasmon. In aluminum, the surface plasmon energy is 10.6 eV, and one sees that the minimum in the dip in the reflectivity occurs near, but below this energy.

We would like to comment on one feature of our calculation, for pure aluminum. In the literature, it is frequently presumed[12,15] that for frequencies above the surface plasmon energy, there is no roughness-induced absorption by the substrate, and as a consequence the roughness-induced change in reflectivity has its origin entirely in the scattering of the incident light away from the specular direction. As we point out earlier,[5] since the imaginary part of the dielectric constant of the substrate is nonzero, there is roughness-induced absorption present at all frequencies, even above the surface plasmon frequency. For the parameters chosen to describe pure aluminum, even at 12 eV we find the dominant contribution to the roughness-induced change in reflectivity comes not from roughness-induced scattering away from the specular direction, but rather from absorption in the substrate. In the calculations reported in the paper by Endriz and Spicer, the roughness-induced scattering rate was found to be considerably larger than that we calculate here. These authors used a considerably larger value of the correlation length ($\approx 1000$ Å) than we have. We find that for larger values of the correlation length, our calculated scattering rate increases appreciably, but we can no longer obtain a reasonable fit to the reflectivity change produced by roughness at lower energies where the surface-plasmon-induced dip occurs.

In Fig. 4, we present our calculations of the roughness-induced change in reflectivity for the replicating-film model described above. One sees that as the thickness of the oxide layer increases, the reflectivity dip shifts toward the visible. The reason for the shift is that the presence of the oxide layer modifies the dispersion relation of the surface plasmon.[16] In particular, for a metal with bulk plasma frequency $\omega_p$, in the limit that the wave vector $k_{\parallel} \to \infty$, the surface plasmon frequency for a metallic substrate overcoated with a dielectric layer with dielectric constant $\epsilon$ approaches the

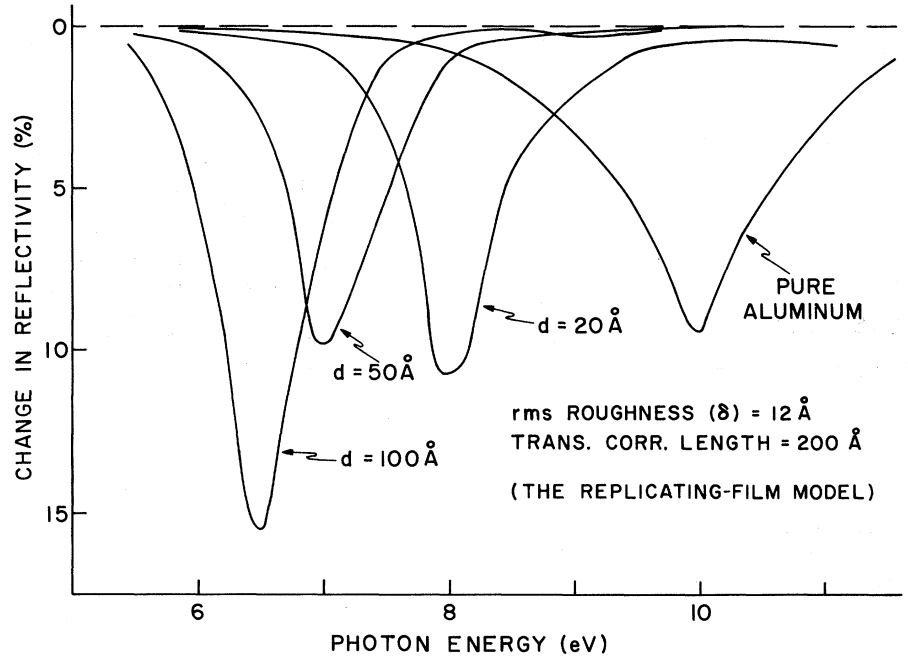


FIG. 4. Change in reflectivity for an aluminum substrate overcoated with oxide films of various thicknesses. The calculations have been carried out for the replicating film model illustrated in Fig. 1(a).

value $\omega_p/(1+\epsilon)^{1/2}$ rather than the value $\omega_p/\sqrt{2}$ associated with the metal-vacuum interface. We would then expect that for large values of the overlayer thickness $d$, the reflectivity dip shifts downward in frequency to lie just below $\omega_p/(1+\epsilon)^{1/2}$. If we choose $\epsilon \simeq 4$ as a typical value for $Al_2O_3$ in the frequency range of interest, then $\omega_p/(1+\epsilon)^{1/2} = 6.7$ eV. Thus, by the time the thickness of the oxide layer reaches 100 Å, the calculations show that the reflectivity dip lies near this asymptotic value.

Note that for the replicating-film model, the magnitude of the dip is not affected by the presence of the overlayer in any dramatic manner.

In Fig. 5, we present calculations of the roughness-induced change in reflectivity for the nonuniform-film model described earlier, and illustrated in Fig. 1 (b). While the position of the

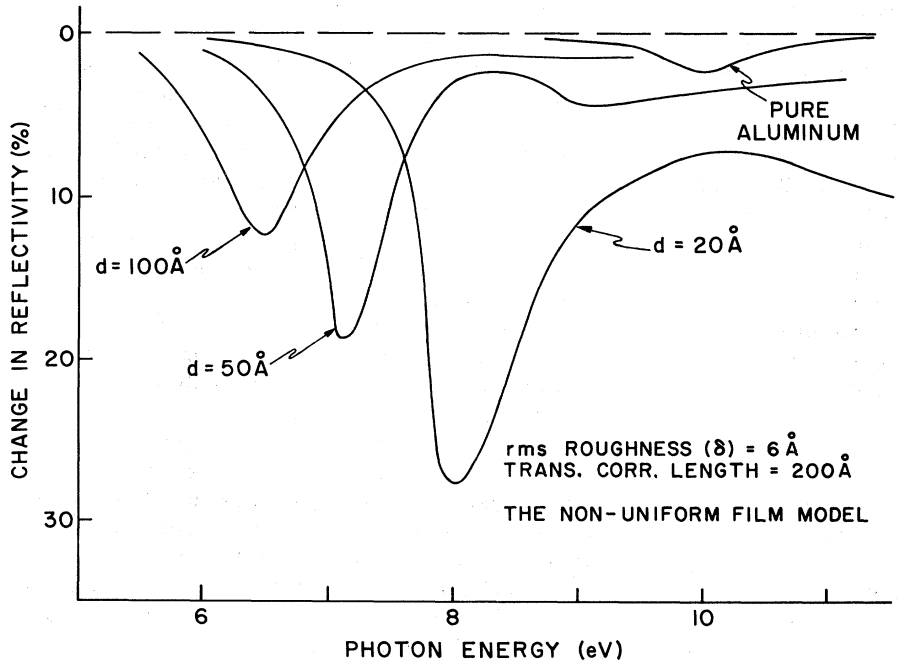


FIG. 5. Change in reflectivity produced by surface roughness, for aluminum overcoated with an oxide film. The calculations have been carried out for parameters given in the figure, and for the nonuniform-film model illustrated in Fig. 1(b).

minimum in the reflectivity for each value of the oxide thickness coincides quite closely with the minima displayed in Fig. 4 for the replicating-film model, the most striking feature of the results in Fig. 5 is the very substantial enhancement of the strength of the coupling between the light and the surface plasmon. Note that in the calculations illustrated in Fig. 5, we have reduced the rms height of the roughness on each interface from the value 12 Å used in Figs. 3 and 4 to the smaller value of 6 Å. Also, note the difference in the scale used on the ordinates in Figs. 4 and 5.

At this point, we may appreciate that the position of the reflectivity minimum is controlled simply by the film thickness, but the strength of the interaction between the incident wave and the surface plasmon is a very sensitive function of the nature of the correlation between the surface roughness on the oxide-vacuum interface, and that on the oxide-substrate interface. The reason for this is the following, if we compare the results in Figs. 4 and 5. When $\zeta_1(x, y) = -\zeta_2(x, y)$, as in the nonuniform-film model, the scattered electromagnetic wave from the oxide-vacuum interface interferes constructively within the oxide film with that which comes from the oxide-substrate interface. This greatly enhances the coupling between the incident radiation and the surface plasmon. Note that in Fig. 5, coupling to the surface plasmon is strongest when $d = 20$ Å. On the same curve, one sees an appreciable change in reflectivity above 9 eV, well above the surface-plasmon-induced reflectivity dip. The large roughness-induced change in the reflectivity above 9 eV comes from energy dissipation within the oxide layer; recall that one is past the absorption edge of the oxide film in this energy range. The constructive interference which produces strong coupling to the surface plasmon thus also leads to considerable absorption within the oxide film in the energy region above its absorption edge. We shall see that in the random-roughness model, where there is no correlation between the roughness on each interface (and hence no constructive interference of the type just described), in the presence of the oxide overlayer, the roughness-induced coupling of the incident radiation to the surface plasmon is still considerably enhanced over the value for the pure aluminum surface, although the magnitude of the enhancement is smaller than for the nonuniform-film model. This means that in the replicating-film model, the two scattered fields evidently interfere destructively, and the enhancement effect provided by the oxide film is supressed as a consequence.

In Fig. 6, we present the results of our calculations for the random-roughness model [Figure 1 (c)]. Again the position of the minimum in the change in reflectivity occurs at the same photon energy as for the replicating-film model. The strength of coupling between the inicident radiation and the surface plasmon is significantly larger than is the case for the pure aluminum surface, although the enhancement factor is considerably smaller in each case than for the nonuniform-film

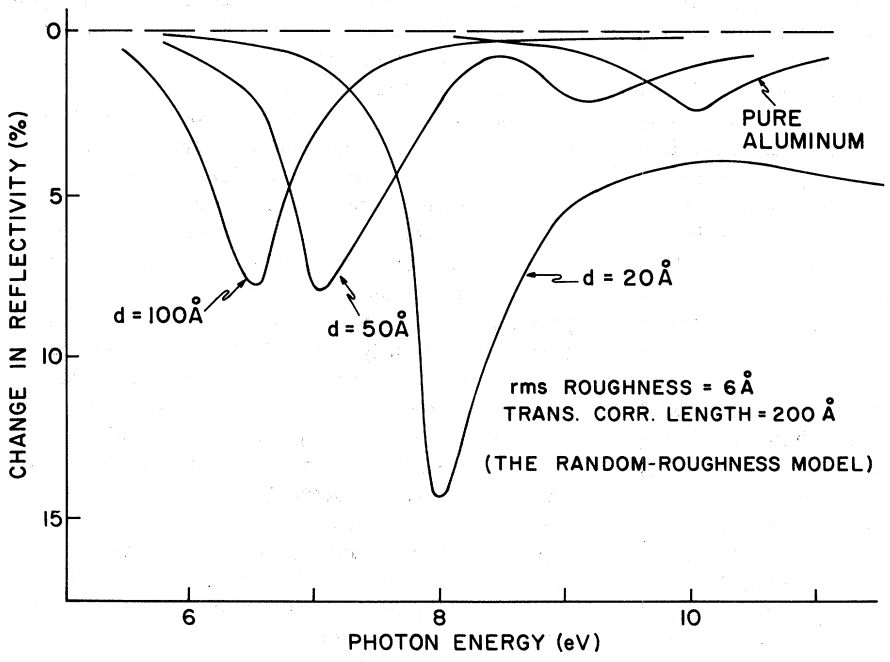


FIG. 6. Change in reflectivity produced by surface roughness, for aluminum overcoated with oxide films of various thickness. The calculations have been carried out for the parameters given in the figure, and for the random-roughness model illustrated in Fig. 1(c).

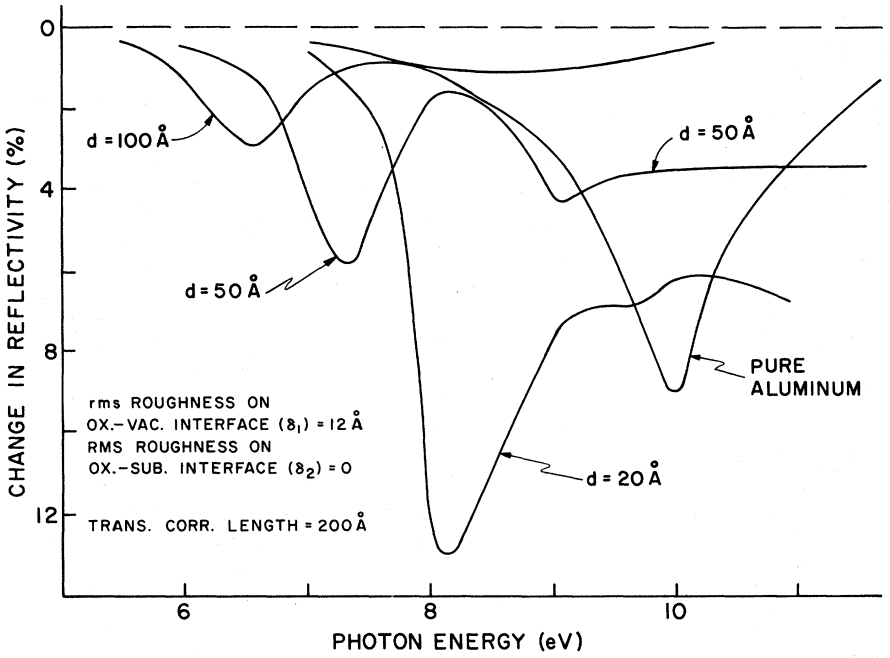


FIG. 7. Change in reflectivity produced by surface roughness, for aluminum overcoated with oxide films of various thickness. The calculations have presumed the oxide-substrate interface is perfectly smooth, with roughness on only the oxide-vacuum interface. The parameters used in the calculation are given on the figure.

model in Fig. 5.

In Fig. 7, we display the results of the calculations for the rough-oxide-layer model. As remarked earlier, we assume here that the oxide-substrate interface is perfectly smooth, but roughness is present on the oxide-vacuum interface. For small values of the oxide-layer thickness, the interaction between the incident radiation and the surface plasmon is enhanced, as in the other two examples where destructive interference does not occur between the scattered fields generated by the pair of rough interfaces. However, as the oxide-layer thickness increases, the strength of the effective coupling eventually begins to decrease. Quite clearly this occurs because the fields associated with the surface plasmon are localized to the inner interface, and as the oxide-layer thickness increases, the rough surface responsible for the reflectivity dip moves sufficiently far from the inner interface to cut off the coupling between the surface plasmons and the incident radiation.

With the results of the above four cases in hand, we make some remarks about the experimental data.

Feuerbacher and Steinman[15] have studied roughness-induced reflectivity dips for aluminum films, and also for roughened films overcoated with 50 Å of LiF. The position of the reflectivity minimum of the roughened aluminum film overcoated with 50 Å of LiF agrees quite well with the calculations presented above. (Of course, our calculations were carried out for aluminum overcoated with aluminum oxide, but in the spectral regime of interest, both LiF and $Al_2O_3$ are transparent, and their dielectric constants do not differ greatly.) If one examines the magnitude of the reflectivity dip they observe, then for the roughened film $\Delta R_{max} \approx 0.25$, while for the overcoated film, $\Delta R_{max} \approx 0.45$. Thus, while the overcoating procedure shifts the reflectivity minimum toward the visible, it does not greatly affect the strength of the roughness-induced coupling of the incident radiation to the surface plasmon. This suggests that the LiF overlayer has roughness on its outer surface which tracks rather closely that on the LiF-substrate interface, as in our replicating-film model of Fig. 1(a).

Stanford and Bennett[17] have studied the effect of overcoating a roughened Ag surface with films $Al_2O_3$ roughly 250 Å thick. They present several measurements in this paper. For a supersmooth uncoated Ag surface, they find a smooth variation of the reflectivity, with no sign of a dip characteristic of roughness-induced coupling to surface plasmons. For an uncoated surface they characterize as "slightly rough," the measured reflectivity tracks that of the supersmooth surface, although a clear hint of a surface plasmon dip is present. The surface-plasmon dip appears as a clear feature in data on a surface they characterize as "relatively rough." When the slightly rough surface is overcoated with $Al_2O_3$, a very large pronounced dip appears. The reflectivity change, only barely visible for the uncoated surface, assumes a maximum of $\approx 0.50$ for the overcoated one. While these measurements are carried out on a

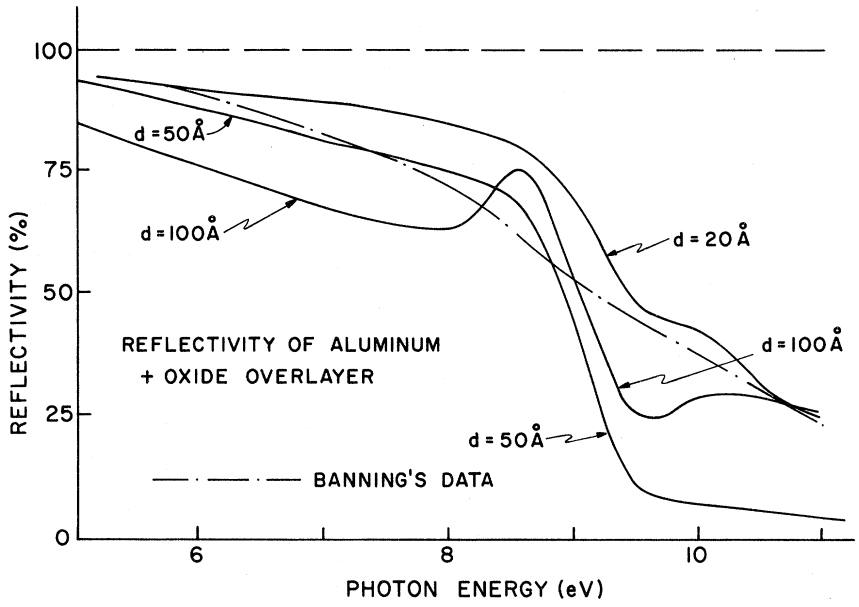


FIG. 8. Reflectivity of an aluminum surface overcoated with oxide in the ultraviolet, for various oxide thicknesses. In these calculations, it is presumed that both interfaces are perfectly smooth.

rather different substrate-overlayer system than that considered here (and also in a different wavelength regime), these data provide a clear example of the behavior illustrated in Figs. 5 and 6, where the overcoating produces an enormous enhancement of the roughness-induced coupling of the incident radiation to the surface plasmon.

The calculations in Fig. 7 suggest that if a supersmooth aluminum surface is overcoated with a dielectric, then if the dielectric layer is sufficiciently thick, the reflectivity of the structure becomes relatively insensitive to the presence of roughness on the outer surface of the overlayer. However, it must be kept in mind that as the thickness of the oxide layer increases, the reflectivity of the structure drops substantially in the ultraviolet even if both interfaces are perfectly smooth, as Ehrenreich has pointed out recently.[18] We illustrate this in Fig. 8, where we present the reflectivity for aluminum overcoated with an oxide layer of uniform thickness, for the case where both interfaces are perfectly smooth. The dot-dashed curve is the data of Banning,[11] which shows a decrease in reflectivity at large photon energies of the sort expected for a surface overcoated with an oxide film. Indeed, the data is fit reasonably by the curve for $d = 20$ Å, for photon energies above 9 eV. It is tempting to suggest that the measured reflectivity drops below the theoretical curve in the region from 7 to 9 eV because of roughness-induced coupling to surface plasmons. However, it is difficult to see how superposition of two distinct mechanisms could produce a curve as smooth and featureless as the data of Banning.

## APPENDIX: CONSTRUCTION OF THE GREEN'S FUNCTIONS FOR THE ELECTROMAGNETIC WAVE EQUATION

In Sec. II of this paper, we introduced a set of Green's functions $D_{\mu\nu}(\vec{x}, \vec{x}'; \omega)$ that satisfy the differential equations

$$\sum_{\mu}\left(\frac{\omega^2}{c^2}\epsilon_0(z,\omega)\delta_{\lambda,\mu} - \frac{\partial^2}{\partial x_\lambda \partial x_\mu} + \delta_{\lambda\mu}\nabla^2\right) D_{\mu\nu}(\vec{x}, \vec{x}'; \omega) = 4\pi\delta_{\lambda\mu}\delta(\vec{x} - \vec{x}') \tag{A1}$$

along with the outgoing-wave boundary conditions appropriate to the present scattering problem. In Eq. (A1), the dielectric function $\epsilon_0(z, \omega)$ is given by Eq. (2.6).

In an Appendix of our preceding paper,[5] we derived the form of these Green's functions for the semi-infinite dielectric, which corresponds to the limit $d \to 0$ in the present geometry. In our preceding paper, we constructed the Green's functions by directly solving the differential equation (A1). This procedure becomes most cumbersome for the present geometry. We present here a much more compact method of constructing the Green's functions.

As in the text, we write

$$D_{\mu\nu}(\vec{x}, \vec{x}'; \omega) = \int \frac{d^2k_\parallel}{(2\pi)^2} e^{i\vec{k}_\parallel \cdot (\vec{x}_\parallel - \vec{x}'_\parallel)} d_{\mu\nu}(\vec{k}_\parallel \omega \mid z z') \tag{A2}$$

and we note that one may write

$$\delta(\vec{x} - \vec{x}') = \delta(z - z') \int \frac{d^2k_\parallel}{(2\pi)^2} e^{i\vec{k}_\parallel \cdot (\vec{x}_\parallel - \vec{x}'_\parallel)}. \tag{A3}$$

With these expressions, one may readily derive a set of one-dimensional coupled differential equa-

tions for the functions $d_{\mu\nu}(\vec{k}_{\parallel}\omega\,|zz')$. These equations simplify considerably if we perform a coordinate rotation which aligns the $\hat{x}$ axis with the direction of $\vec{k}_{\parallel}$. This is achieved by the action of the matrix

$$\underline{S}(\vec{k}_{\parallel}) = \frac{1}{k_{\parallel}} \begin{pmatrix} k_x & k_y & 0 \\ -k_y & k_x & 0 \\ 0 & 0 & k_{\parallel} \end{pmatrix}. \tag{A4}$$

We introduce a new set of functions $g_{\mu',\nu'}(k_{\parallel}\omega\,|zz'')$ related to $d_{\mu}(k_{\parallel}\omega\,|zz')$ by the rotation just described:

$$d_{\mu\nu}(\vec{k}_{\parallel}\omega\,|zz') = \sum_{\mu'\nu'} g_{\mu',\nu'}(k_{\parallel}\omega\,|zz')\, S_{\mu',\mu}(\vec{k}_{\parallel})\, S_{\nu',\nu}(\vec{k}_{\parallel}). \tag{A5}$$

It is a straightforward matter to construct the equations obeyed by the functions $g_{\mu\,\nu}(k_{\parallel}\omega\,|zz')$. These equations read

$$\left(\epsilon_0(z,\omega)\frac{\omega^2}{c^2} - k_{\parallel}^2 + \frac{d^2}{dz^2}\right) g_{yy}(k_{\parallel}\omega\,|zz') = 4\pi\delta(z-z'), \tag{A6}$$

$$\left(\epsilon_0(z,\omega)\frac{\omega^2}{c^2} + \frac{d^2}{dz^2}\right) g_{xx}(k_{\parallel}\omega\,|zz') - ik_{\parallel}\frac{dg_{zx}(k_{\parallel}\omega\,|zz')}{dz} = 4\pi\delta(z-z'), \tag{A7}$$

$$-ik_{\parallel}\frac{d}{dz}g_{xx}(k_{\parallel}\omega\,|zz') + \left(\epsilon_0(z,\omega)\frac{\omega^2}{c^2} - k_{\parallel}^2\right) \times g_{zx}(k_{\parallel}\omega\,|zz') = 0, \tag{A8}$$

$$\left(\epsilon_0(z,\omega)\frac{\omega^2}{c^2} + \frac{d^2}{dz^2}\right) g_{xz}(k_{\parallel}\omega\,|zz') - ik_{\parallel}\frac{d}{dz}g_{zz}(k_{\parallel}\omega\,|zz') = 0, \tag{A9}$$

$$-ik_{\parallel}\frac{d}{dz}g_{xz}(k_{\parallel}\omega\,|zz') + \left(\epsilon_0(z,\omega)\frac{\omega^2}{c^2} - k_{\parallel}^2\right) g_{zz}(k_{\parallel}\omega\,|zz') = 4\pi\delta(z-z'). \tag{A10}$$

The remaining functions ($g_{xy}$, $g_{yx}$, $g_{yx}$, $g_{zy}$) obey homogeneous equations, and thus vanish identically.

We begin with $g_{yy}(k_{\parallel}\omega\,|zz')$, since Eq. (A6) is uncoupled with the remaining four equations. We first observe that for a medium characterized by the $z$-dependent dielectric constant $\epsilon_0(z,\omega)$, Maxwell's equations yield solutions of the form

$$\vec{E}(k_{\parallel}\omega\,|\vec{x}) = \hat{y}E_y(k_{\parallel}\omega\,|z)\,e^{ik_{\parallel}x}, \tag{A11}$$

where $E_y(k_{\parallel}\omega\,|z)$ obeys the homogeneous version of Eq. (A6):

$$\left(\epsilon_0(z,\omega)\frac{\omega^2}{c^2} - k_{\parallel}^2 + \frac{d^2}{dz^2}\right) E_y(k_{\parallel}\omega\,|z) = 0. \tag{A12}$$

There are two linearly independent solutions of the differential equation (A12). We denote the two solutions by $E_y^{>}(k_{\parallel}\omega\,|z)$, and $E_y^{<}(k_{\parallel}\omega\,|z)$, where we choose the functions to satisfy the boundary conditions

$$\lim_{z\to+\infty} E_y^{>}(k_{\parallel}\omega\,|z) = e^{+ik_0 z} \tag{A13a}$$

and

$$\lim_{z\to-\infty} E_y^{<}(k_{\parallel}\omega\,|z) = e^{+ik_2 z}, \tag{A13b}$$

where we define the quantities

$$k_{1,2} = \left(\frac{\omega^2}{c^2}\epsilon_{1,2} - k_{\parallel}^2\right)^{1/2}, \quad \mathrm{Im}(k_{1,2}) < 0 \tag{A14a}$$

$$k_0 = \left(\frac{(\omega+i\eta)^2}{c^2} - k_{\parallel}^2\right)^{1/2}, \quad \mathrm{Im}(k_0) > 0. \tag{A14b}$$

In Eq. (A14a), we presume $\epsilon_1$ and $\epsilon_2$ have a positive, nonzero imaginary part, and for the proper square root to be chosen for $k_0$, we have added a positive imaginary infinitesimal $i\eta$ to the frequency. The limit $\eta \to 0$ is always to be taken in Eq. (A14b).

The Green's function $g_{yy}(k_{\parallel}\omega\,|zz')$ is to be constructed so that Eq. (2.11) describes a scattered wave which radiates into the vacuum for $z > d$, and one that attenuates in the region $z < 0$. This Green's function is simply expressed in terms of $E_y^{>}(k_{\parallel}\omega\,|z)$ and $E_y^{<}(k_{\parallel}\omega\,|z)$ as follows[20]:

$$g_{yy}(k_{\parallel}\omega\,|zz') = \frac{4\pi}{W_{\perp}(k_{\parallel},\omega)}\left[E_y^{>}(k_{\parallel}\omega\,|z)\,E_y^{<}(k_{\parallel}\omega\,|z')\theta(z-z') + E_y^{<}(k_{\parallel}\omega\,|z)\,E_y^{>}(k_{\parallel}\omega\,|z')\,\theta(z'-z)\right], \tag{A15}$$

where

$$W_{\perp}(k_{\parallel},\omega) = \frac{\partial E_y^{>}(k_{\parallel}\omega\,|z)}{\partial z}E_y^{<}(k_{\parallel}\omega\,|z) - \frac{\partial E_y^{<}(k_{\parallel}\omega\,|z)}{\partial z}E_y^{>}(k_{\parallel}\omega\,|z), \tag{A16}$$

is the Wronskian, a quantity independent of $z$.[20]

The form given in Eq. (A15) is valid for any function $\epsilon_0(z,\omega)$. For the particular geometry of concern here, where $\epsilon_0(z,\omega)$ is given by Eq. (2.6), it is a straightforward exercise to construct these two functions. One has

$$E_y^{>}(k_{\parallel}\omega\,|z) = \begin{cases} e^{+ik_0 z}, & z > d \\ A_+^{(1)}e^{ik_1 z} + A_-^{(1)}e^{-ik_1 z}, & 0 < z < d \\ B_+^{(1)}e^{ik_2 z} + B_-^{(1)}e^{-ik_2 z}, & z < 0 \end{cases} \tag{A17}$$

and

$$E_y^{<}(k_{\parallel}\omega\,|z) = \begin{cases} D_+^{(1)}e^{ik_0 z} + D_-^{(1)}e^{-ik_0 z}, & z > d \\ C_+^{(1)}e^{ik_0 z} + C_-^{(1)}e^{-ik_1 z}, & 0 < z < d \\ e^{ik_2 z}, & z < 0 \end{cases} \tag{A18}$$

where in these expressions, with $\sigma = +$ or $-$,

$$A_\sigma^{(\perp)} = \frac{e^{ik_0 d}}{2}\left(1+\sigma\frac{k_0}{k_1}\right)e^{-i\sigma k_1 d}, \tag{A19}$$

$$B_\sigma^{(\perp)} = \frac{e^{ik_0 d}}{2}\left[\left(1+\sigma\frac{k_0}{k_1}\right)\cos(k_1 d) - i\left(\frac{k_0}{k_1}+\sigma\frac{k_1}{k_2}\right)\sin(k_1 d)\right], \tag{A20}$$

$$C_\sigma^{(\perp)} = \frac{1}{2}\left(1+\sigma\frac{k_2}{k_1}\right), \tag{A21}$$

$$D_\sigma^{(\perp)} = \frac{e^{ik_0 d}}{2}\left[\left(1+\sigma\frac{k_2}{k_0}\right)\cos(k_1 d) + i\left(\frac{k_2}{k_1}+\sigma\frac{k_1}{k_0}\right)\sin(k_1 d)\right], \tag{A22}$$

and the Wronskian is given by

$$W_\perp(k_\parallel,\omega) = (e^{ik_0 d}/k_1)\left[(k_1^2 - k_2 k_0)\sin(k_1 d) + i(k_0 - k_2)k_1\cos(k_1 d)\right]. \tag{A23}$$

The functions $g_{xx}(k_\parallel\omega\,|\,zz')$ and $g_{zx}(k_\parallel\omega\,|\,zz')$ obey the coupled equations (A7) and (A8). These functions may be constructed by generalizing the method used to obtain $g_{yy}(k_\parallel\omega\,|\,zz')$.

We begin by noting that if we seek a solution of Maxwell's equations in the form

$$\vec{\mathbf{E}}(k_\parallel\omega\,|\,\vec{\mathbf{x}}) = \{\hat{x}E_x(k_\parallel\omega\,|\,z) + \hat{z}E_z(k_\parallel\omega\,|\,z)\}e^{ik_\parallel x}, \tag{A24}$$

then the functions $E_x(k_\parallel\omega\,|\,z)$ and $E_z(k_\parallel\omega\,|\,z)$ satisfy the coupled equations

$$\left(\epsilon_0(z,\omega)\frac{\omega^2}{c^2}+\frac{d^2}{dz^2}\right)E_x(k_\parallel\omega\,|\,z) - ik_\parallel\frac{d}{dz}E_z(k_\parallel\omega\,|\,z) = 0, \tag{A25}$$

$$-ik_\parallel\frac{d}{dz}E_x(k_\parallel\omega\,|\,z) + \left(\epsilon_0(z,\omega)\frac{\omega^2}{c^2} - k_\parallel^2\right)E_z(k_\parallel\omega\,|\,z) = 0. \tag{A26}$$

For the geometry under consideration here, where $\epsilon_0(z,\omega)$ is piecewise constant, we must have $\nabla\cdot\vec{\mathbf{E}} = 0$ everywhere except at the singular points $z=0$ and $z=d$. This requires (except at the two points)

$$\frac{d}{dz}E_z(k_\parallel\omega\,|\,z) + ik_\parallel E_x(k_\parallel\omega\,|\,z) = 0. \tag{A27}$$

Thus, if we are given $E_z(k_\parallel\omega\,|\,z)$, then from Eq. (A27) we may compute $E_x(k_\parallel\omega\,|\,z)$ in each regime of interest. We confine our attention to $E_z(k_\parallel\omega\,|\,z)$ as a consequence.

There are two linearly independent sets of solutions of the system of equations from Eq. (A25) through Eq. (A27), just as when we examined Eq. (A25). We append the superscript $>$ to the set $E_x^>(k_\parallel\omega\,|\,z)$, $E_z^>(k_\parallel\omega\,|\,z)$ for which $E_z^>(k_\parallel\omega\,|\,z)$ obeys the boundary condition

$$\lim_{z\to+\infty} E_z^>(k_\parallel\omega\,|\,z) = e^{+ik_0 z}, \tag{A28}$$

and we append the superscript $<$ to the set for which

$$\lim_{z\to-\infty} E_z^<(k_\parallel\omega\,|\,z) = e^{-ik_2 z}. \tag{A29}$$

Before we proceed, we display the explicit form of the fields $E_{x,z}^>(k_\parallel\omega\,|\,z)$ and $E_{x,z}^<(k_\parallel\omega\,|\,z)$. One has

$$\begin{aligned} E_z^>(k_\parallel\omega\,|\,z) &= e^{ik_0 z}, && z>d\\ &= A_+^{(\parallel)}e^{ik_1 z} + A_-^{(\parallel)}e^{-ik_1 z}, && 0<z<d\\ &= B_+^{(\parallel)}e^{ik_2 z} + B_-^{(\parallel)}e^{-ik_2 z}, && z<0 \end{aligned} \tag{A30}$$

$$\begin{aligned} E_x^>(k_\parallel\omega\,|\,z) &= -(k_0/k_\parallel)e^{ik_0 z}, && z>d\\ &= -(k_1/k_\parallel)(A_+^{(\parallel)}e^{ik_1 z} - A_-^{(\parallel)}e^{-ik_1 z}), && 0<z<d\\ &= -(k_2/k_\parallel)(B_+^{(\parallel)}e^{ik_2 z} - B_-^{(\parallel)}e^{-ik_2 z}), && z<0 \end{aligned} \tag{A31}$$

and

$$\begin{aligned} E_z^<(k_\parallel\omega\,|\,z) &= D_+^{(\parallel)}e^{ik_0 z} + D_-^{(\parallel)}e^{-ik_0 z}, && z>d\\ &= C_+^{(\parallel)}e^{ik_1 z} + C_-^{(\parallel)}e^{-ik_1 z}, && 0<z<d\\ &= e^{ik_2 z}, && z<0 \end{aligned} \tag{A32}$$

$$\begin{aligned} E_x^<(k_\parallel\omega\,|\,z) &= -(k_0/k_\parallel)(D_+^{(\parallel)}e^{ik_0 z} - D_-^{(\parallel)}e^{-ik_0 z}), && z>d\\ &= -(k_1/k_\parallel)(C_+^{(\parallel)}e^{ik_1 z} - C_-^{(\parallel)}e^{-k_1 z}), && 0<z<d\\ &= -(k_2/k_\parallel)e^{ik_2 z}, && z<0. \end{aligned} \tag{A33}$$

In these expressions, one has, with $\sigma = +$ or $-$,

$$A_\sigma^{(\parallel)} = \frac{1}{2}\left(\frac{1}{\epsilon_1}+\sigma\frac{k_0}{k_1}\right)e^{ik_0 d}e^{-i\sigma k_1 d}, \tag{A34}$$

$$B_\sigma^{(\parallel)} = e^{ik_0 d}\left[\left(\frac{1}{\epsilon_2}+\sigma\frac{k_0}{k_2}\right)\cos(k_1 d) - i\left(\frac{k_0\epsilon_1}{k_1\epsilon_2}+\sigma\frac{k_1}{\epsilon_1 k_2}\right)\sin(k_1 d)\right], \tag{A35}$$

$$C_+^{(\parallel)} = \frac{1}{2}\left(\frac{\epsilon_2}{\epsilon_1}+\sigma\frac{k_2}{k_1}\right), \tag{A36}$$

$$D_+^{(\parallel)} = \frac{e^{ik_0 d}}{2}\left[\left(\epsilon_2+\sigma\frac{k_2}{k_0}\right)\cos(k_1 d) + i\left(\epsilon_1\frac{k_2}{k_1}+\sigma\frac{k_1\epsilon_2}{k_0\epsilon_1}\right)\sin(k_1 d)\right]. \tag{A37}$$

Given the fields defined in Eq. (A30)–(A33), we seek solutions of Eq. (A7) and Eq. (A8) in the form

$$g_{xx}(k_\parallel\omega\,|\,zz') = \frac{4\pi}{W_\parallel(k_\parallel,\omega)}\left[E_x^>(k_\parallel\omega\,|\,z)E_x^<(k_\parallel\omega\,|\,z')\Theta(z-z') + E_x^<(k_\parallel\omega\,|\,z)E_x^>(k_\parallel\omega\,|\,z')\Theta(z'-z)\right] \tag{A38}$$

and

$$g_{zx}(k_\parallel\omega\,|\,zz') = \frac{4\pi}{W_\parallel(k_\parallel,\omega)}\left[E_z^>(k_\parallel\omega\,|\,z)E_x^<(k_\parallel\omega\,|\,z')\Theta(z-z') + E_z^<(k_\parallel\omega\,|\,z)E_x^>(k_\parallel\omega\,|\,z')\Theta(z'-z)\right]. \tag{A39}$$

Substitution of these forms into Eq. (A7) and Eq. (A8) show that the solution indeed has the form of

Eq. (A38) and Eq. (A39) if we choose

$$W_{\parallel}(k_{\parallel}, \omega) = W_{xx}(k_{\parallel}, \omega) - W_{zz}(k_{\parallel}, \omega), \tag{A40}$$

where $W_{xx}(k_{\parallel}, \omega)$ and $W_{zz}(k_{\parallel}, \omega)$ are given by Eq. (A18), but with $y$ replaced by $x$ or $z$.

Explicit calculation shows that for our geometry $W_{xx}(k_{\parallel}, \omega)$ and $W_{zz}(k_{\parallel}, \omega)$ are only piecewise constant; i.e., these functions are constant everywhere, but experience jump discontinuities at $z=0$ and $z=d$. However, the function $W_{\parallel}(k_{\parallel}, \omega)$ is truly constant, with a value everywhere given by

$$W_{\parallel}(k_{\parallel}, \omega) = \frac{\omega^2 k_0}{ic^2 k_{\parallel}^2} e^{ik_0 d}\left[\left(\epsilon_2 - \frac{k_2}{k_0}\right)\cos(k_1 d) + i\left(\epsilon_1 \frac{k_2}{k_1} - \frac{\epsilon_2 k_1}{\epsilon_1 k_0}\right)\sin(k_1 d)\right]. \tag{A41}$$

Thus, we have left only the two functions $g_{zz}(k_{\parallel}\omega \,|\, zz')$ and $g_{xz}(k_{\parallel}\omega \,|\, zz')$. If we attempt to search for a solution of Eq. (A9) and Eq. (A10) by constructing the direct analogs of Eq. (A38) and Eq. (A39), we shall find the resulting functions fail to satisfy Eq. (A9) and Eq. (A10). We recall that when we explicitly constructed the Green's functions in Ref. 5, we found that $g_{zz}$ contained a term directly proportional to $\delta(z-z')$. Thus, we look for a solution of the form

$$g_{xz}(k_{\parallel}\omega \,|\, zz') = -\frac{4\pi}{W_{\parallel}(k_{\parallel}, \omega)}[E_x^{>}(k_{\parallel}\omega \,|\, z)E_z^{<}(k_{\parallel}\omega \,|\, z')\Theta(z-z') + E_x^{<}(k_{\parallel}\omega \,|\, z)E_z^{>}(k_{\parallel}\omega \,|\, z')\Theta(z'-z)] \tag{A42}$$

for $g_{xz}$, but for $g_{zz}$ we take

$$g_{zz}(k_{\parallel}\omega \,|\, zz') = \Gamma(z')\delta(z-z') - \frac{4\pi}{W_{\parallel}(k_{\parallel}, \omega)}[E_z^{>}(k_{\parallel}\omega \,|\, z)E_z^{<}(k\omega \,|\, z')\Theta(z-z') + E_z^{<}(k_{\parallel}\omega \,|\, z)E_z^{>}(k_{\parallel}\omega \,|\, z')\Theta(z'-z)]. \tag{A43}$$

This form indeed solves the differential equation with $W_{\parallel}(k_{\parallel}, \omega)$ given by Eq. (A40) and Eq. (A41) provided we choose

$$\Gamma(z') = 4\pi c^2/\omega^2 \epsilon_0(z', \omega). \tag{A44}$$

We now have the explicit form for all the Green's functions required for the calculation of the scattered fields in each region of interest.

---

*Supported in part by Contract No. DAHC15-73-C-0127 of the Advanced Research Projects Agency of the Department of Defense, and in part by Grant No. AFOSR 71-2018 of the Air Force Office of Scientific Research, Office of Aerospace Research, U.S.A.F.

[1]For example, see the experimental data reported by J. Endriz and W. Spicer [Phys. Rev. B 4, 4144 (1971)] along with the discussion presented by these authors.

[2]See the data on aluminum films deposited on fire-polished substrates reported by B. P. Feuerbacher and W. Steinmann, Opt. Commun. 1, 81 (1969).

[3]J. L. Stanford and H. E. Bennett, Appl. Opt. 8, 2556 (1969).

[4]J. L. Stanford, J. Opt. Soc. Am. 60, 49 (1970).

[5]A. A. Maradudin and D. L. Mills, Phys. Rev. B (to be published).

[6]H. Froitzheim, H. Ibach and D. L. Mills, report (unpublished).

[7]For example, see the discussion in Chapter XIX of A. Messiah, *Quantum Mechanics* (North-Holland, Amsterdam, 1962), Vol. II.

[8]To obtain Eq. (2.15), one needs to evaluate integrals of the form $\int dz'\, F(z')\,\delta(z'-z_0)$ where here $z_0$ is either 0 or $d$. For the case of normal incidence considered, all functions $F(z')$ encountered are continuous at the point $z'=z_0$ where the argument of the $\delta$ function vanishes, in contrast to the functions encountered in Ref. 5, when the case where incident radiation that strikes the surface at non-normal incidence was also considered. Thus, in the present case, the integral over $z'$ may be evaluated in an unambiguous matter, to produce results in accord with those obtained by matching fields across the displaced boundaries.

[9]The definition of $\varphi_s$ used here differs from that in Ref. 5. The two are related by a 90° rotation, so $\sin^2\varphi_s$ appears here where $\cos^2\varphi_s$ appeared previously, and conversely.

[10]E. T. Arakawa and M. W. Williams, J. Phys. Chem. Solids 29, 735 (1968).

[11]H. Ehrenreich, H. R. Phillipp, and B. Segall, Phys. Rev. 132, 1918 (1963).

[12]J. G. Endriz and W. E. Spicer, Phys. Rev. B 4, 4144 (1971).

[13]J. M. Elson and R. H. Ritchie, Phys. Rev. B 4, 4129 (1971).

[14]J. M. Elson and R. H. Ritchie, Phys. Stat. Sol. (to be published).

[15]B. P. Feuerbacher and W. Steinman, Opt. Commun. 1, 81 (1969).

[16]For example, see the work of J. J. Cowan and E. T. Arakawa, Phys. Stat. Sol. 1, 695 (1970).

[17]J. L. Stanford and H. E. Bennett, Appl. Opt. 8, 2556 (1969).

[18]H. Ehrenreich, report (unpublished).

[19]M. Banning, J. Opt. Soc. Am. 32, 98 (1942).

[20]See the discussions in Chap. 8 of B. Friedman, *Principles and Techniques of Applied Mathematics* (Wiley, New York, 1956).